ARTICLE

Chirality Effects in Atomic Vacancy-Limited Transport in Metallic Carbon Nanotubes

Hui Zeng,[†,‡,⊥] Huifang Hu,[†] and Jean-Pierre Leburton[‡,§,*]

[†]College of Material Science and Engineering, College of Physics and Microelectronic Science, Hunan University, Changsha 410082, China, [‡]Beckman Institute, and [§]Department of Electrical and Computer Engineering, Department of Physics, University of Illinois at Urbana—Champaign, Urbana, Illinois 61801. [⊥]Current address: College of Physical Science and Technology, Yangtze University, Jingzhou 434023, China.

ABSTRACT We use first principles density functional theory combined with nonequilibrium Green's function technique to investigate the electronic and transport properties of metallic armchair and zigzag carbon nanotubes (CNTs) with different kinds of multivacancy defects. While the existence of a small band gap in pristine zigzag (12,0) CNTs lowers its conductance compared to pristine armchair (7,7) CNTs, transport properties in the presence of multi (hexa)-vacancy are superior in the former nanostructure, that is more sensitive to defect size and topology than the latter. In addition, in the zigzag structures hexavacancy nanotubes have higher conductance than divancancy nanotubes, which is due to the presence of midgap states that reduce the transmission gap and enhance the conductance.

KEYWORDS: carbon nanotubes · quantum transport · defects · simulation

Single walled carbon nanotubes (SWNTs) have attracted continued interest since their discovery in 1993, due to their outstanding physical properties.[1,2] In this context, extensive experimental efforts[1] have been developed to investigate the kinetics of atomic-scale defect formation in the nanostructure,[3,4] since defects play a decisive influence on their electronic, transport, and mechanical properties.[5] High-resolution transmission electron microscopy (TEM) studies have shown clear evidence of the presence of point defects such as monovacancy,[6,7] interstitial-vacancy defects,[8] and pentagon-heptagon defects[9] in carbon nanotubes (CNTs) and graphene. More recently, Florian reported the possibility of artificially creating individual vacancies in carbon nanostructures by using an electron beam of 1 Å diameter.[10] Although the presence of vacancies deteriorates the genuine properties of nanotubes, in term they may have beneficial effects,[11] as for instance, a dangling bond can provide active sites for atomic adsorption,[12] which can be used as catalysts for thermal dissociation of water.[13]

While considerable theoretical works have been devoted to the understanding of the electronic properties of carbon nanotubes with monovacancies[14] and divacancies,[15] transport properties in the presence of clusters of vacancies have received little attention.[16] Such studies are timely since small holes of a few atoms feature sizes that have recently been created in metallic carbon nanotubes with diameter of about 10 nm,[17] as clearly evidenced by scanning tunneling microscopy. It was also shown that higher-order defects can be formed by removing a group of atoms with high energy impacts[7] or chemical etching.[18] Among the important fundamental and technological issues related to the formation of vacancy clusters are the influences of defect size and their spatial symmetry as well as the CNT chirality on the transport properties.

In this communication, we investigate the electronic and transport properties of zigzag and armchair CNTs in the presence of mono-, di- and hexavacancy defects. For this purpose, we focus on (12,0) and (7,7) nanostructures as both are metallic with different chiralities, where the former (zigzag) is known to develop a small band gap of the order of ~50 to 70 meV (semimetallic),[19] whereas the latter (armchair) is gapless around the Fermi level.[20] We use density functional theory to assess the stability of each structure with atomic vacancies subjected to the formation of new bonds during reconstruction estimated from energetic and structural considerations.[21] Quantum transport properties in the stable nanostructures are then computed by means of the nonequilibrium Green's function technique.[22] Our most striking result is the different conductance behavior be-

*Address correspondence to jleburto@illinois.edu.

Received for review September 9, 2009 and accepted November 23, 2009.

Published online December 10, 2009. 10.1021/nn901192g

tween zigzag and armchair nanotubes with atomic vacancy sizes. Indeed, while conductance in the (7,7) CNT is monotonously decreasing with increasing defect size, the conductance in the hexavacancy (12,0) CNT is larger than the divacancy nanostructures. We attribute this different behavior to the presence of the gap in the zigzag CNT. In both cases, different hexavacancy configurations have different influences on the conductance.

MODEL

We simulate two metallic (12,0) and (7,7) single wall CNTs (SWNTs) with 10 Å diameter by using a supercell of length $L \approx 42$ Å. We perform optimization calculations using the density functional theory, as implemented in the SIESTA code.[23] The standard norm-conserving Troullier−Martins[24] pseudopotential orbitals are used to calculate the ion−electron interaction. We use the numerical double-ζ plus polarization (DZP) basis set, and plane cutoff energy is chosen as 200 Ry. The exchange correction term is calculated within the generalized gradient approximation.[25] To test the accuracy of the structure of defected tube after reconstruction, we compare our relaxed structures with published works and found good agreement.[15,16]

To compute the transport properties of the defective CNTs, we consider a two-probe geometry system[26] constructed in such a way that the central region consists of an optimized supercell (contains 10 unit cells for (12,0) nanotube and 17 unit cells for (7,7) nanotube) containing the defects, which is surrounded by two leads made of one unit pristine supercell on each side. Our band-structure calculations for both structures are shown to be consistent with previous works[27,28] and ensure that our results are reliable. More details about the NEGF formalism can be found in ref 22. The current is calculated by means of the Laudauer formula:

$$I = \frac{2e}{h}\int_{\mu_{min}}^{\mu_{max}} dE(f_l - f_r)T(E, V_b) \qquad (1)$$

where the transmission coefficient T as a function of the electron energy E is given by

$$T(E, V_b) = 4Tr[Im(\Sigma^l G^R \Sigma^r G^A)] \qquad (2)$$

Σ^l (Σ^r) represents the self-energies of the left (right) electrode, G^R (G^A) is retard (advanced) Green's function, f_l (f_r) is the corresponding electron distribution function of the electron eigenstates of the left (right) electrode. Furthermore, $\mu_{min} = \min(\mu + V_b, \mu)$ [$\mu_{max} = \max(\mu + V_b, \mu)$] denotes the minimum (maximum) electrochemical potential μ of the electrodes. The calculations are performed at $T = 300$ K.

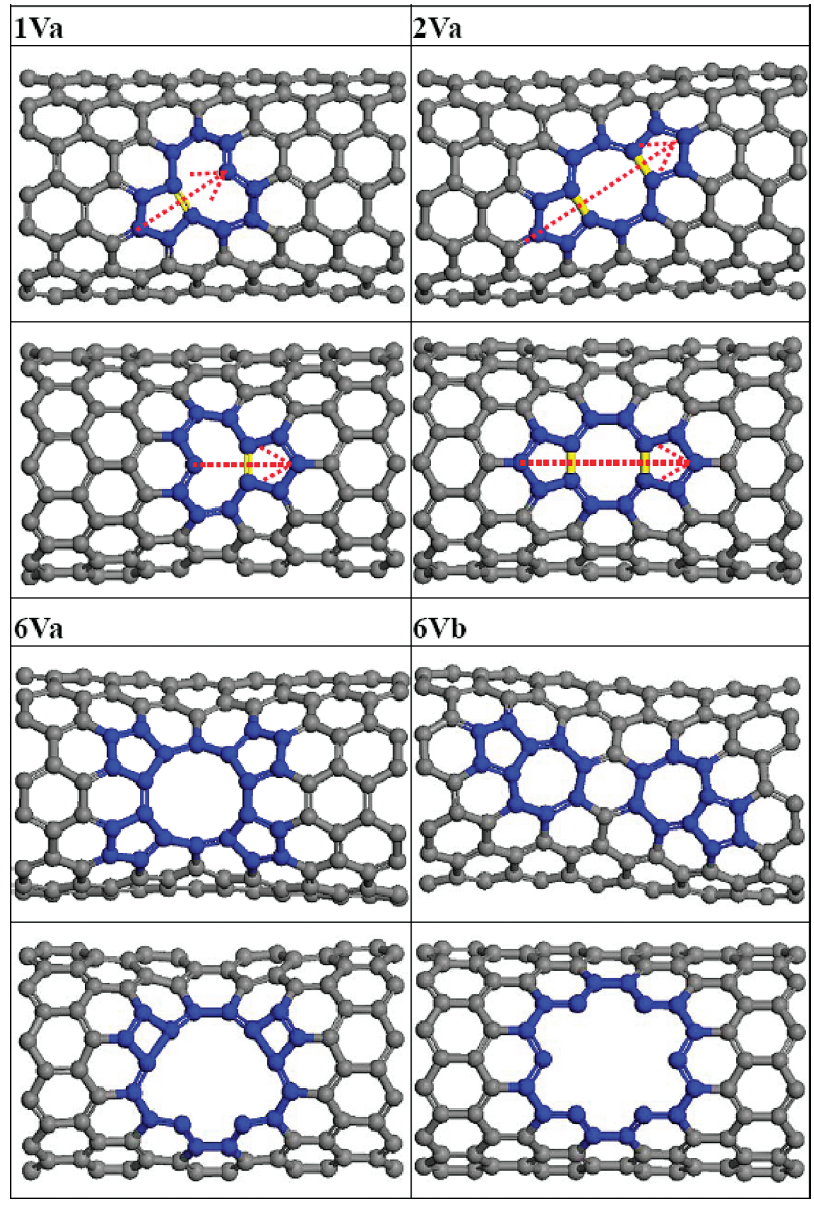

Figure 1. Vacancy configurations of all structural models. (a and b) Ball-and-stick model for (7,7) and (12,0) SWNT with monovacancy, divacancy and hexavacancy, respectively. The newly formed C−C bonds during the reconstruction are highlighted by yellow, and the atoms at the far side are omitted for clarity.

TABLE 1. Transformation Energy E_f

configuration	(7,7) SWNT	(12,0) SWNT
1Va	6.41 eV	5.85 eV
2Va	3.57 eV	3.69 eV
6Va	9.41 eV	21.31 eV
6Vb	6.97 eV	18.97 eV

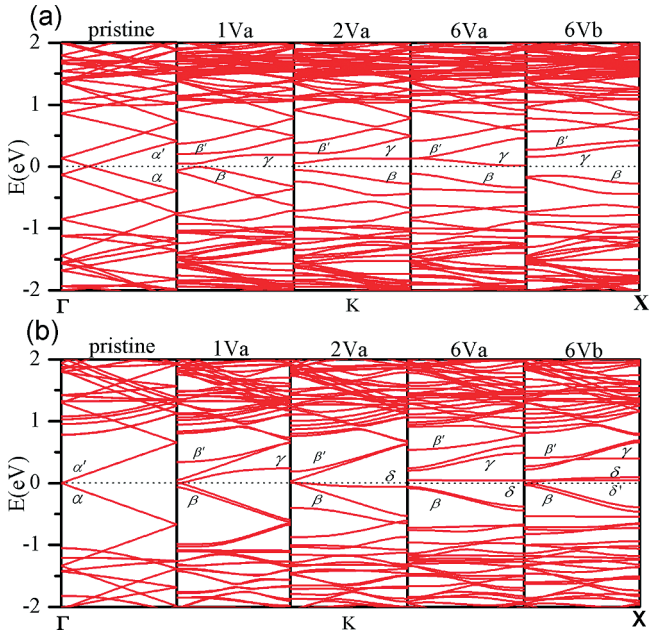

Figure 2. Band structure of (a) (7,7) and (b) (12,0) SWNT with various vacancies. The band structure of the pristine nanotube is also given for comparison.

RESULTS AND DISCUSSION

Figure 1 shows different stable or metastable configurations of carbon vacancies, that is, mono- (1Va), di- (2Va), and hexavacancy (6Va, 6Vb) in armchair and zigzag SWNTs obtained after structural optimization by SIESTA. The optimization process is performed by spontaneously reconstructing the CNT around the defects; Table 1 lists the transformation energy for all configurations.[29] Generally, the reconstruction around the monovacancy (1Va) defect gives rise to a dangling bond (DB) and leaves a so-called 5−1DB defect.[30,31] This dangling bond can provide an active site for atomistic adsorption. The 5−1DB defect is one of the most stable structures. Note that the orientations of the 5−1DB defect in (7,7) and (12, 0) SWNTs are different. In this framework, we define the defect orientation as the angle made by the axis of defect (indicate by the red arrowed in Figure 1) with the horizontal direction. Hence, the 5−1DB defect in the (7,7) SWNT is titled at 38° with respect to the axis, while the orientation of the 5−1DB defect in the (12,0) SWNT is parallel to the tube axis, which is a consequence of the CNT chirality. In the situation of divacancies (2Va), the optimization process shows that four uncoordinated carbon nanotubes around the missing carbon atoms have bonded together, forming a pentagon−octagon−pentagon (5−8−5) defect. We also observe that the orientation of the 5−8−5 defect in the (7,7) SWNT is titled by 32° with respect to the axis while it remains parallel to the axis in (12,0) SWNT. It is worth mentioning that the 5−8−5 defect is the most stable defect because of its lowest transformation energy (see Table 1).[4] For the hexavacancy clusters, our simulation shows that the (7,7) nanotubes have the lowest formation energies. For this armchair nanostructures, the hexavacancy configurations do not contain any unsaturated atoms, unlike zigzag (12,0) CNTs, for which the 6Va configuration exhibit two unsaturated atoms compared with six unsaturated carbon atoms in the 6Vb configuration. Except for the 6Vb defect in the armchair (7,7) nanotube, all configurations manifest as a large hole in the tube. Specifically, in the (12,0) nanotube, the 6Va configuration contains a symmetric tetra-decagon (14-bond ring) and the 6Vb configuration manifests as a missing hexagon that results in six unsaturated carbon atoms. The transformation energy of the hexavacancy configurations are the largest, as shown in Table 1, suggesting that the large holes may split into smaller size vacancies through atomic reconstruction. The lowest transformation energy for the hexa-vacancies occurs for the 6Vb configuration in the (7,7) nanotube, made of two 5−7 defects separated by a hexagon. This configuration is associated with atomic bond shrinking around the defects area, where bonds perpendicular to the nanotube axis are more affected due the CNT curvature. Overall, it can be seen that all defects only affect the local structure of the SWNT, whereas the diameter of the structure near the defect shrinks accordingly.

The electronic band structure of the two types of nanotubes with various defect configurations and their pristine analogues are displayed in Figure 2. In the band structure of the pristine (7,7) nanotube, the highest occupied band α and the lowest unoccupied band α' cross at the Fermi level, away from the Γ-point. In the armchair 1Va configuration, the titled 5−1DB defect creates a state-labeled γ that appears above the Fermi level, and results from quasi-bound unsaturated σ-orbitals.[14] This γ-state hybridizes with the α,α'-bands to evolve into the β,β'-bands that anticross at the Fermi level close to the Γ-point. The γ-band is now the lowest unoccupied band[32] which anticross with the β-band opening the direct band gap of about 0.05 eV. In the 2Va configuration, the γ-state has moved closer to the Fermi level. The reconstruction process of

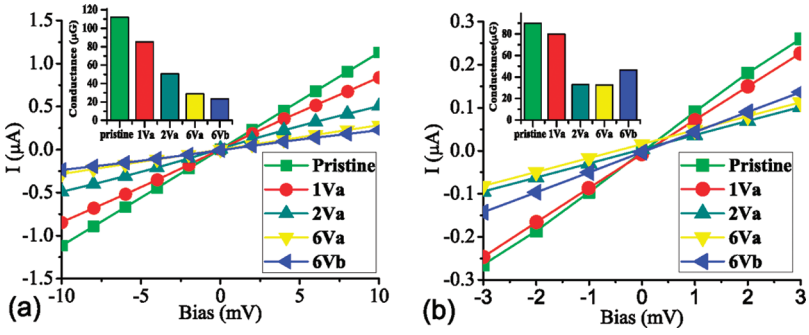

Figure 3. *I*−*V* curve and conductance (inset map) of (a) (7,7) and (b) (12,0) defective SWNT, the result of pristine is given for comparison. The same color in *I*−*V* curve and in conductance (inset map) denotes the same structure.

the tilted divacancy has introduced twisting-type deformations and opened a band gap of about 0.11 eV at the Γ-point, which is consistent with previous work.[15] Except for the anticrossing of the low β-band close to the X-point (*ca.* −0.6 eV), the band structure away from the Fermi level does not experience much change; therefore, the large scale deformation (5−8−5 defects) dominates the electronic structure of the tilted divacancies nanostructure. In the 6Va configuration, the split β,β′-bands move away from the Fermi level significantly, while the γ-state approaches the Fermi level, especially close to the X-point. This roll-off at large *k* vectors effectively reduces the band gap and makes the current in this configuration a little larger than in the 6Vb case (see Figure 3). The band gap of the 6Vb configuration is further increased to 0.325 eV, as β,β′- and γ-bands move apart. Overall, it can be seen that the band gap in the various vacancy configurations of the (7,7) SWNTs is monotonously increasing with the increasing numbers of atomic vacancy (or the size of the vacancy cluster).

In the pristine (12,0) nanotube, the α,α′-bands converge at the Γ-point; both are doubly degenerate and contribute to two quantum transmission channels. Finer scale simulation however reveals a small band gap due to the curvature effect.[19] In the presence of vacancy defects, the doubled degenerate α,α′-bands split at the Γ-point and become the modified β,β′-bands. In the 1Va structure, the defect introduces a γ-state that results from quasi-bound unsaturated σ-orbitals,[14] as in the (7,7) SWNT. It crosses the β-band at the Γ-point, and is partially occupied around the symmetry point at the expense of the β′-bands. In the 2Va nanotube, the band structure resembles the 1Va structure with a larger splitting of the β-bands at the Γ-point. Here, there is a new state called δ, very close and below the Fermi level with a very small dispersion that flattens near the X-point, also predicted by Berber *et al.*[15] The existence of a large hole in the 6Va configuration opens the band gap by moving the β,β′-bands apart, and the δ-state is now very flat and above the Fermi level, while the γ-band reappears. The band structure resembles the one in the 6Vb configuration of the (12,0) CNTs but with δ-state. The 6Vb vacancy that consists of a large hole in the nanotube produces a new defect state labeled δ′, very close to its parent δ-state, above the Fermi level.

Figure 3 shows the $I - V$ characteristics of the two sets, that is, (7,7) and (12,0), of carbon nanotubes, with the corresponding conductances for each vacancy size and configuration in insets. The voltage range corresponds to an electric field range of 15 KV/cm, for which all $I-V$ characteristics are linear with the applied voltage. For both chiralities, the conductance of the pristine nanotube is the highest, closely followed by the 1Va conductance, indicating that the 5−1DB defect does not remarkably scatter electrons. Also, as expected the conductances of the pristine armchair (7,7) nanostructures are higher than the pristine zigzag (12,0) CNTs because of the absence of transmission gap in the former. The conductance of the divacancy (7,7) nanotube is the second highest due to the (5−8−5) defects that gives rise to significant electron backscattering, and translate into a decrease of the transmission coefficient larger than the 1Va CNT. The conductance continues to decrease in the 6Va (7,7) nanostructures, because backscattering increases compared with the 2Va case. Finally, the 6Vb (7,7) configuration has the lowest conductance because of the smaller transmission coefficient at the Fermi level compared with that of the 6Va CNT. Generally speaking, the (7,7) nanotube conductance is a monotonic function of the defect size and geometry.

In the (12,0) CNTs, the drop in the conductance of the divacancy nanostructure is slightly deeper than in the 2Va (7,7) CNTs, which we attribute to the presence of the localized δ-state close to the Fermi level in the former. Unexpectedly, the conductance of both hexavacancy (12,0) configurations is equal or superior to that of the divacancy (12,0) nanotube. Indeed, both defects have a highly symmetric pattern that reduces the curvature effect compared with the divacancy structure, and thereby reduces the transmission gap, which in the 6Va configuration boosts the conductance to a level comparable to the 2Va CNTs. In the 6Vb (12,0) structure this effect is enhanced by the presence of the β,β′-bands, which also enhances the transmission around the gap. This defect is spatially more symmetric than the 6Va vacancy, which reduces backscattering compared to the latter. Moreover, the topology of the defect is directly responsible for the higher conductance of the 6Vb (12,0) CNT compared to its analogue in the armchair (7,7) CNT, as the band gap in the former is even smaller than in the latter structure. The curvature effect can be clearly seen in comparing the distortion produced by the 6Vb defect on both the armchair and zigzag structures in Figure 1. The anomalous conductance variation in the (12,0) nanotubes shows that the transport in a defective CNT is not a direct function of the number of missing atoms but of the chirality and defect pattern in the nanostructure.

CONCLUSION

In this communication, we have shown unexpected conductance variations between armchair and zigzag metallic carbon nanotubes in the presence of multivacancy defects. Specifically, conductance in zigzag CNTs is not a monotonic function of the number of missing C-atoms compared with the conductance of armchair metallic CNTs. In the former, the conductance depends on the reconstruction around the defect and its spatial symmetry. Our results suggest the ability to tailor the atomic structure of carbon nanotubes and provide new ways to control their transport properties.

Acknowledgment. The authors thank Prof. A. Bezryadin, T. Markussen, Dr. J. W. Wei, and Ph.D. Y. Xu for fruitful discussion. We also acknowledge technical assistance from T. Markussen and M. A. Kuroda. Extensive calculations are performed in the MAC OS X Turing cluster. This work is supported by National Basic Research Program Grant No. 2006CB921605. Hui Zeng would like to thank the China Scholarship Council and the Beckman Institute for supporting his study in the University of Illinois at Urbana−Champaign as a joint Ph.D. candidate.

REFERENCES AND NOTES

1. Iijima, S.; Ichihashi, T. *Nature* **1993**, *263*, 603–605.
2. Saito, R.; Dresselhaus, G.; Dresselhaus, M. S. *Physical Properties of Carbon Nanotubes*; Imperial College Press: London, 1998.
3. Telling, R. H.; Ewels, C. P.; El-Barbary, A. A.; Heggie, M. I. *Nat. Mater.* **2004**, *2*, 333–337.
4. Amorim, R. G.; Fazzio, A.; Antonelli, A.; Novaes, F. D.; da Silva, A. J. R. *Nano Lett.* **2007**, *7*, 2459–2462.
5. Ajayan, P. M.; Ravikumar, V.; Charlier, J. C. *Phys. Rev. Lett.* **1998**, *81*, 1437–1440.
6. Hashimoto, A.; Suenaga, K.; Gloter, A.; Urita, K.; Iijima, S. *Nature* **2004**, *43*, 870–873.
7. Jin, C.; Suenaga, K.; Iijima, S. *Nano Lett* **2008**, *8*, 1127–1130.
8. Urita, K.; Suenaga, K.; Sugai, T.; Shinohara, H.; Iijima, S. *Phys. Rev. Lett.* **2005**, *94*, 105502.
9. Suenaga, K.; Wakabayashi, H.; Koshino, M.; Sato, Y.; Urita, K.; Iijima, S. *Nat. Nanotechnol.* **2007**, *2*, 358–360.
10. Rodriguez-Manzo, J. A.; Banhart, F. *Nano Lett.* **2009**, *9*, 2285–2289.
11. Krasheninnikov, A. V.; Banhart, F. *Nat. Mater.* **2007**, *6*, 723–733.
12. Terrones, M.; Terrones, H.; Banhart, F.; Charlier, J.-C.; Ajayan, P. M. *Science* **2000**, *288*, 1226–1229.
13. Kostov, M. K.; Santiso, E. E.; George, A. M.; Gubbins, K. E.; Nardelli, M. B. *Phys. Rev. Lett.* **2005**, *95*, 136105.
14. Choi, H. J.; Ihm, J.; Louie, S. G.; Cohen, M. L. *Phys. Rev. Lett.* **2000**, *84*, 2917–2920.
15. Berber, S.; Oshiyama, A. *Phys. Rev. B* **2008**, *77*, 165405.
16. Kotakoski, J.; Krasheninnikov, A. V.; Nordlund, K. *Phys. Rev. B* **2006**, *74*, 245420.
17. Aref, T.; Remeika, M.; Bezryadin, A. *J. Appl. Phys.* **2008**, *104*, 024312.
18. Zobelli, A.; Gloter, A.; Ewels, C. P.; Colliex, C. *Phys. Rev. B* **2008**, *77*, 045410.
19. Ouyang, M.; Huang, J.-L.; Cheung, C. L.; Lieber, C. M. *Science* **2001**, *292*, 702–705.
20. Kane, C. L.; Mele, E. J. *Phys. Rev. Lett.* **1997**, *78*, 1932–1935.
21. Jones, R. O.; Gunnarsson, O. *Rev. Mod. Phys.* **1989**, *61*, 689–746.
22. Datta, S. *Quantum Transport: Atom to Transistor*; Cambridge University Press: New York, 2005.
23. (a) Ordejón, P.; Artacho, E.; Soler, J. M. *Phys. Rev. B* **1996**, *53*, R10441–R10444. (b) Soler, J. M.; Artacho, E.; Gale, J. D.; García, A.; Junquera, J.; Ordejón, P.; Sánchez-Portal, D. *J. Phys.: Condens. Matter* **2002**, *14*, 2745–2779.
24. Troullier, N.; Martins, J. L. *Phys. Rev. B* **1993**, *43*, 1993–2006.
25. Perdew, J. P.; Burke, K.; Ernzerhof, M. *Phys. Rev. Lett.* **1996**, *77*, 3865–3868.
26. (a) Taylor, J.; Guo, H.; Wang, J. *Phys. Rev. B* **2001**, *63*, 245407. (b) Brandbyge, M.; Mozos, J.-L.; Ordejón, P.; Taylor, J.; Stokbro, K. *Phys. Rev. B* **2003**, *65*, 165401.
27. Yamamoto, T.; Nakazawa, Y.; Watanabe, K. *New J. Phys.* **2007**, *9*, 245.
28. Rocha, A. R.; Padilha, J. E.; Fazzio, A.; da Silva, A. J. R. *Phys. Rev. B* **2008**, *77*, 153406.
29. The transformation energy E_f is defined as $E_f = E_d - N_d/N_p \times E_p$, where E_d is the total energy of the defective tube, E_p is the total energy of the pristine tube, and N_d and N_p are the number of the atoms in the defective tube and pristine tube, respectively.
30. Lu, A. J.; Pan, B. C. *Phys. Rev. Lett.* **2004**, *92*, 105504.
31. Rossato, J.; Baierle, R. J.; Fazzio, A.; Mota, R. *Nano Lett.* **2005**, *5*, 197–200.
32. We simulated the band structure for the SWNT configurations with different number of cells (CNT lengths) and found no qualitative change among them. The only difference is that the δ-state becomes flattened with increasing CNT length.